Assessment of Impacts of Climate Change on Runoff from Nuranang Watershed of Arunachal Pradesh

S. Rajkumari*, N. Chiphang, A. Bandyopadhyay and A. Bhadra
Department of Agricultural Engineering, North Eastern Regional Institute of Science and Technology, Itanagar, Arunachal Pradesh, India
Corresponding author email id: shelianna07@gmail.com

Abstract: The present study evaluated the impact of climate change on runoff from the Nuranang watershed. HadCM3 model had been employed for emission scenarios of A2 and B2. The downscaled maximum, minimum temperatures, and daily precipitation using SDSM for the baseline (1979–2009) and future time period, i.e., 2011–2040 (2020s), 2041–2070 (2050s), and 2071–2099 (2080s) were computed and compared. The projected change in maximum temperature (T_{max}) and minimum temperature (T_{min}) showed an increasing trend in the future years under A2 and B2 scenarios. Under both the scenarios A2 and B2, the PA (average precipitation) were found to be decreasing in 2050s compared to 2020s, then from 2050s, it increased in 2080s. The predicted changes in total runoff as computed using SDSRM were observed as -0.81%, -3.22%, and 21.21% under A2 scenario and 7.46%, -4.27%, and 15.20% under B2 scenario for the future years 2020s, 2050s, and 2080s, respectively.
Keywords: Climate change, Runoff, SDSM, SDSRM

1. Introduction

Climate change is a serious global environmental concern. IPCC (2014) has reported that the globally averaged combined land and ocean surface temperature showed a warming of 0.85 °C over the period 1880 to 2012. The annual mean temperature is reported to be increased by 0.01 °C per year in the eastern Himalayas (Shrestha and Devkota, 2010). Runoff from snow covered area is considerably different from exposed land as, after rainfall, the runoff from exposed land contributes immediately as compared to snow covered area, where the snow needs to ripe before it melts and contributes to stream flow. Accurate estimation of the volume of water stored in the snow pack and its rate of release is essential to predict the flow during the snowmelt period (Raghunath, 2006). In order to compute climate change in the snow dominated watershed, it is essential to stimulate snowmelt flow from precipitation and temperature data derived from General Circulation Models (GCM) outputs corresponding to the specific climate change scenarios, using a suitable hydrological model. However, the spatial resolutions of GCMs are usually quite coarse (hundred kilometers) which results in the loss of regional and local details of the climate that are influenced by spatial heterogeneities missing from these models (Schubert and Sellers, 1997). Therefore, spatial downscaling methods can convert the GCM outputs into at least a reliable daily rainfall and temperature time series at the scale of the watershed for which the hydrological impact is going to be investigated. The statistical model that is very popular in GCM downscaling is Statistical Downscaling Model (SDSM) developed by Wilby and Wilks (1999) and Wilby et al. (2002). Many studies (Wilby et al., 1998; Harpam and Wilby, 2005; Dibike and Coulibaly, 2005; Fowler et al., 2007) have suggested that SDSM is simple and easy to handle and thus have been widely used.

The assessment of hydrologic response to climate change is required in watershed management and planning to protect water resources and environment equality. In the recent years, several hydrological models have been used for assessment of impacts of climate change on hydrological processes. Liu et al., 2011 calibrated and validated semi distributed hydrological model (SWAT) to study the impact of climate change in streamflow in the Yellow river basin. Using the outputs from global circulation model (HadCM3), SDSM and a combination of "bilinear-interpolation and delta" were applied to generate daily time series of temperature and precipitation (1961–2099). The generated data was integrated to simulate streamflow under current and future climate conditions. Kabiri et al., 2015 provided downscaled meteorological variables corresponding to the Hadley Centre Third Generation-GCM model for emission scenarios A2 and B2 for the period 2001–2100 as input using SDSM and calibrated and validated Hydrologic Engineering Center's Hydrologic Modeling System (HEC-HMS) hydrological model to simulate the corresponding future streamflow changes in the Klang watershed in Malaysia.

The present study aims at assessing the impacts of potential future climatic changes on the hydrology of the catchment area of Nuranang watershed situated at Tawang district of Arunachal Pradesh, India. In this paper, the degree day model: Spatially Distributed Snowmelt Runoff Model (SDSRM) was selected to simulate snowmelt runoff of the study area. A downscaling of the meteorological variables obtained as output from the Hadley Centre Coupled Model version 3 (HadCM3) GCM for Special Report on Emissions Scenarios (SRES) A2 and B2 scenarios was performed using SDSM, a regression-based downscaling tool. The downscaled meteorological variables were then incorporated to the present observed data to evaluate the changes in runoff under the projected future climate.

2. Study Area and Methods

Study area

Nunarang watershed located in Tawang district of Arunachal Pradesh, India was selected as the study site. It has an area of 53 km^2 and its map is shown in Fig. 1. The Nuranang river originates from Sela lake and joins Tawang river as Nuranang fall at Jang. The altitude of the Sela Lake is 4,211 m above mean sea level (MSL) and it lies at 27° 30' 15" N and 92° 06' 16" E. The Central Water Commission (CWC) discharge site at RA III, Jang (27° 33' 01" N and 92° 01' 13" E) (Fig. 1) was selected as the outlet point with an elevation of 3,459 m above MSL. Elevation of the watershed ranges from 3,459 to 4,892 m above MSL with an average slope of 51%. At upper elevations, climate is alpine and at lower elevations, it is temperate. Latitude ranges from 27° 30' to 27° 35' N, whereas longitude ranges from 92° 00' to 92° 07' E. Having an average annual precipitation of 1,139 mm, monsoon season stretches from May to September. Snowfall starts from late October and ends in March. Melting of snow starts from February and completely depletes by early June. Snow accumulation and ablation periods vary with years. The entire watershed is dominated by seasonal snow cover.

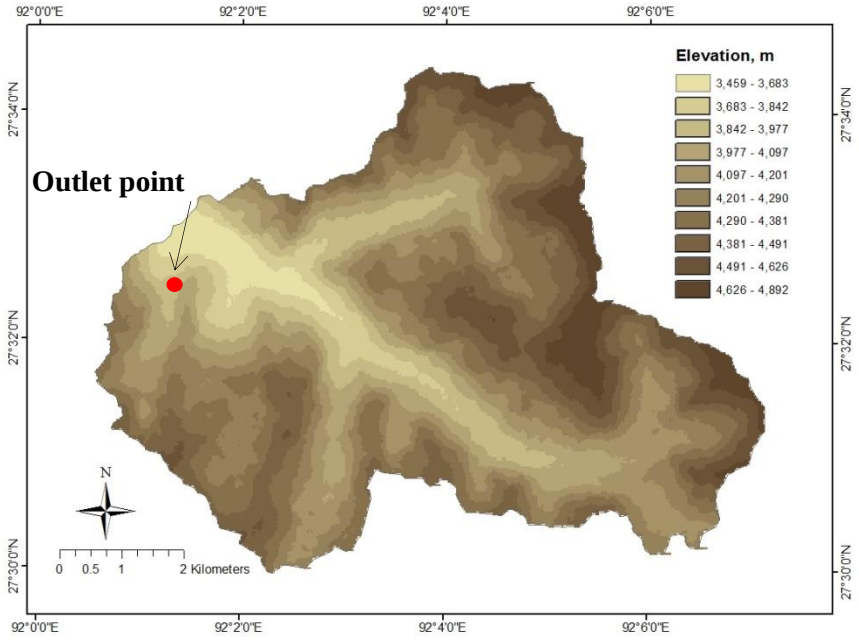

Fig. 1: Nuranang watershed and its gauging site

Data used

Meteorological and hydrological data

The meteorological and hydrological data for Nurarang watershed from 2004, 2005, 2008 and 2009 measured at CWC discharge site at RA-III, Tawang district were collected from CWC office, Itanagar, Arunachal Pradesh, India.

Satellite and other data

The list of satellite and other data required for the study is give n in Table 1.

Table 1 List of data acquired for the present study

Sl. No.	Parameters	Type	Source
1.	Snow cover (500 m resolution)	Spatial	MODIS (http://reverb.echo.nasa.gov/reverb/)
2.	Maximum and minimum air temperatures (T_{max} and T_{min})	Time series	CWC
3.	Precipitation (P)	Time series	CWC
4.	Latitude	Spatial (Static)	Generated
5.	Longitude	Spatial (Static)	Generated
6.	Critical temperature (T_{CRIT})	Time series (Static)	Calibrated
7.	DEM	Spatial (Static)	ASTER

8.	Mean temperature	Spatial	Generated from T_{max} and T_{min}
9.	Lapse rate	Constant	Bandyopadhyay et al. (2014)
10.	Albedo (500 m resolution)	Spatial	MODIS (http://reverb.echo.nasa.gov/)
11.	LULC	Spatial (Static)	Space Application Center (SAC)
12.	Proportion of rain to snow in last storm	Spatial	Generated from T_{CRIT}
13.	Days since cessation of storm	Spatial	Generated from Precipitation
14.	Day of year	Time series	Generated from date

Pre-processing of data

The study area is in the eastern part of Arunachal Pradesh which falls within the bounding box 91–98° E and 26–30° N and it is in h26v06 tiles. Native MODIS data files are stored in HDF-EOS, therefore, MODIS Reprojection Tool (MRT) (Version 4.1) was used for converting downloaded data from HDF-EOS to GeoTIFF format for GIS software. Using ARC MAP 2010, the MODIS snow cover and albedo geotiff data were reprojected to Universal Transverse Mercator (UTM) projection with geographic coordinate system of GCS_WGS_1984. DEM raster downloaded from ASTER was resample using ARC MAP 2010 in order to obtained each pixel of same resolution with the other MODIS data layer. By selecting the outlet point, Nuranang basin was delineated from DEM. The basin was then represented by the number of grids or pixels of equal size. Then, the data was clipped and converted into ASCII format using ARC MAP 2010.
The downloaded observed data for operation of SDSM were in numerical control file format (nc) so these data were converted to geotiff format using Qgis software which was downloaded from http://www.qgis.org/en/site/. The resultant raster images were clipped using ArcMap. The extraction of time series for temperature (maximum and minimum) and precipitation were also done using Arcmap.

Hydrological Modelling using SDSRM

The spatially distributed snowmelt runoff model (SDSRM), developed by Department of Agricultural Engineering, NERIST (Itanagar), is based on temperature index approach which equates the total daily melt to degree day factor times the temperature difference between the mean daily temperature and a base temperature. Temperature index model assumes that there is a linear empirical relationship between air temperature and rate of snowmelt. Two approaches are used in SDSRM to determined snowmelt runoff and they are Temperature index algorithm and modified Temperature index algorithm or Radiation-temperature index

algorithm. In the present study, temperature index algorithm was used. Snow albedo, fractional snow cover, daily maximum temperature, daily minimum temperature, daily precipitation, latitude, longitude, LULC, and DEM are the minimum input layers required for temperature index algorithm. In addition to these layers, incoming shortwave solar radiation is required for modified temperature index algorithm. Runoff coefficient for snowmelt (c_S), runoff coefficient for rain (c_R), lapse rate and critical temperature (T_{CRIT}) are the input coefficient required in the model. The parameter such as proportion of rain to snow in last storm, days since the cessation of storm, mean temperature and day of year are calculated within the model. The model gives pixel-wise output of Snow Density, Snow Depth, Snow water Equivalent, Degree Day, Net Solar radiation, Evaporation, SCA curve, Hypsometric curve, Snow Melt Depth, Rain-induced runoff, Snow-induce runoff, Total runoff, Total Loss and Infiltration.
Calibration of the model was done for depletion period of 2004 and 2005, while the validation was performed for the depletion period of 2008 and 2009.

Statistical Downscaling using SDSM 4.2.9

Statistical DownScaling Model (SDSM) 4.2.9 is a Windows based decision support tool that establishes empirical relationships between GCM-resolution climate variables and local climate. Quality control check in SDSM is perform on the observed predictands, i.e., precipitation (P) and temperatures (T_{max} and T_{min}) to identify errors and missing records in the data. In the screen variables process, the predictors were selected. SDSM performs three tasks: seasonal correlation analysis, partial correlation analysis, and scatterplots. The significance level was used to test the significance of predictor-predictand correlations. SDSM also reports partial correlations between the selected predictors and the predictand. The result screen gives two values, i.e., partial r (partial correlation) and p (probability). Only those predictors having values of partial r within -1 to 1 and p value near to 0 are chosen. From *Scatter* menu, inter-variable behaviour for specified sub-periods (annual, seasonal or monthly) was visually inspected. The appropriate predictor variables that had strong correlation with the predictand variable were identified.

The *Calibrate* Model takes up each of the predictand and a set of probable predictors and computes the parameters of multiple regression equations by using an optimization algorithm (ordinary least squares). For model calibration, the period from 1979–1995 was chosen. The given period was chosen for calibration as both the observed predictands and NCEP predictors were available. In model calibration, initially, the potential predictors which had shown the best correlations with precipitation and temperatures was introduced to the downscaling model. Once the explained variance and SE values obtained are found satisfactory, the regression model is finalized. The *validation* process followed the model calibration. The same parameters used during the calibration process that explains the statistical agreement between the observed and simulated data were used for validation. The period from 1996–2001 was used to validate the performance of the model. The performance of SDSM on validating data was evaluated based on the coefficient of determination (R^2) and

standard error of estimate (SEE). The *Scenario Generator* operation was applied for both the A2 and B2 emission scenarios from the HadCM3 experiment for the period 1961–2099 to predict future climate forcing. The A2 and B2 emission scenarios were downloaded for the period from 1969–2099. The maximum and minimum temperatures and daily precipitation for the baseline (1979–2009) and future time slices, i.e., 2011–2040 (2020s), 2041–2070 (2050s), and 2071–2099 (2080s) were computed and compared.

Assessment of impacts of climate change using the hydrological model

The downscaled projected values for the future scenarios, i.e., 2011–2040 (2020s), 2041–2070 (2050s), 2071–2097 (2080s) including the baseline period (1979–2009) under A2 and B2 scenarios for maximum temperature, minimum temperatures and precipitation were derived using the *Scenario Generator* of SDSM. The scenario generator of SDSM gives 20 ensembles of daily temperatures (maximum and minimum) and precipitation values for the baseline period and all the future time slices under A2 and B2 scenarios. Monthly average temperatures (maximum and minimum) and precipitation values of all the time slices for the two scenarios were calculated from the daily values. The month-wise change in °C for maximum temperature and minimum temperature and change in % for precipitation for each future time slices corresponding to the baseline period were determined. From this, the annual average of the month-wise changed values of the maximum temperature (T_{max}), minimum temperature (T_{min}) and precipitation (P) for the time slices 2020s, 2050s and 2080s under both A2 and B2 emission scenarios were determined for the 20 ensembles of SDSM. The maximum, minimum and mean value from the 20 ensembles of annually averaged month-wise changed values of the temperatures (maximum and minimum) and precipitation were determined. The maximum, minimum and average change of T_{max} (°C) were denoted as TMx, TMn and TA, respectively. The maximum, minimum and average change of T_{min} (°C) were denoted as tMx, tMn and tA, respectively. Also, the maximum, minimum and average change of P (%) were denoted as PMx, PMn and PA, respectively. Thus, 27 different combinations of TMx, TMn, TA, tMx, tMn, tA, PMx, PMn and PA were established for the future time slices 2020s, 2050s and 2080s under both A2 and B2 scenarios as shown in Table 2.

The changed values in T_{max}, T_{min} and P under the A2 and B2 scenarios were incorporated with the daily observed average maximum temperature, minimum temperature and precipitation values of the simulation years 2004, 2005, 2008 and 2009. Considering these changed values, runoff from the Nuranang watershed were simulated using calibrated and parameterized SDSRM for all 27 combinations for each of the six cases (three future periods 2020s, 2050s and 2080s, and two scenarios A2 and B2).

Table 2 Different combinations of future changes in temperature and precipitation

A2 2020	A2 2050	A2 2080	B2 2020	B2 2050	B2 2080
A2TMxtMxPMx20	A2TMxtMxPMx50	A2TMxtMxPMx80	B2TMxtMxPMx20	B2TMxtMxPMx50	B2TMxtMxPMx80
A2TMxtMxPMn20	A2TMxtMxPMn50	A2TMxtMxPMn80	B2TMxtMxPMn20	B2TMxtMxPMn50	B2TMxtMxPMn80
A2TMxtMxPA20	A2TMxtMxPA50	A2TMxtMxPA80	B2TMxtMxPA20	B2TMxtMxPA50	B2TMxtMxPA80
A2TMxtMnPMx20	A2TMxtMnPMx50	A2TMxtMnPMx80	B2TMxtMnPMx20	B2TMxtMnPMx50	B2TMxtMnPMx80
A2TMxtMnPMn20	A2TMxtMnPMn50	A2TMxtMnPMn80	B2TMxtMnPMn20	B2TMxtMnPMn50	B2TMxtMnPMn80
A2TMxtMnPA20	A2TMxtMnPA50	A2TMxtMnPA80	B2TMxtMnPA20	B2TMxtMnPA50	B2TMxtMnPA80
A2TMxtAPMx20	A2TMxtAPMx50	A2TMxtAPMx80	B2TMxtAPMx20	B2TMxtAPMx50	B2TMxtAPMx80
A2TMxtAPMn20	A2TMxtAPMn50	A2TMxtAPMn80	B2TMxtAPMn20	B2TMxtAPMn50	B2TMxtAPMn80
A2TMxtAPA20	A2TMxtAPA50	A2TMxtAPA80	B2TMxtAPA20	B2TMxtAPA50	B2TMxtAPA80
A2TMntMxPMx20	A2TMntMxPMx50	A2TMntMxPMx80	B2TMntMxPMx20	B2TMntMxPMx50	B2TMntMxPMx80
A2TMntMxPMn20	A2TMntMxPMn50	A2TMntMxPMn80	B2TMntMxPMn20	B2TMntMxPMn50	B2TMntMxPMn80
A2TMntMxPA20	A2TMntMxPA50	A2TMntMxPA80	B2TMntMxPA20	B2TMntMxPA50	B2TMntMxPA80
A2TMntMnPMx20	A2TMntMnPMx50	A2TMntMnPMx80	B2TMntMnPMx20	B2TMntMnPMx50	B2TMntMnPMx80
A2TMntMnPMn20	A2TMntMnPMn50	A2TMntMnPMn80	B2TMntMnPMn20	B2TMntMnPMn50	B2TMntMnPMn80
A2TMntMnPA20	A2TMntMnPA50	A2TMntMnPA80	B2TMntMnPA20	B2TMntMnPA50	B2TMntMnPA80
A2TMntAPMx20	A2TMntAPMx50	A2TMntAPMx80	B2TMntAPMx20	B2TMntAPMx50	B2TMntAPMx80
A2TMntAPMn20	A2TMntAPMn50	A2TMntAPMn80	B2TMntAPMn20	B2TMntAPMn50	B2TMntAPMn80
A2TMntAPA20	A2TMntAPA50	A2TMntAPA80	B2TMntAPA20	B2TMntAPA50	B2TMntAPA80
A2TAtMxPMx20	A2TAtMxPMx50	A2TAtMxPMx80	B2TAtMxPMx20	B2TAtMxPMx50	B2TAtMxPMx80
A2TAtMxPMn20	A2TAtMxPMn50	A2TAtMxPMn80	B2TAtMxPMn20	B2TAtMxPMn50	B2TAtMxPMn80
A2TAtMxPA20	A2TAtMxPA50	A2TAtMxPA80	B2TAtMxPA20	B2TAtMxPA50	B2TAtMxPA80
A2TAtMnPMx20	A2TAtMnPMx50	A2TAtMnPMx80	B2TAtMnPMx20	B2TAtMnPMx50	B2TAtMnPMx80
A2TAtMnPMn20	A2TAtMnPMn50	A2TAtMnPMn80	B2TAtMnPMn20	B2TAtMnPMn50	B2TAtMnPMn80
A2TAtMnPA20	A2TAtMnPA50	A2TAtMnPA80	B2TAtMnPA20	B2TAtMnPA50	B2TAtMnPA80
A2TAtAPMx20	A2TAtAPMx50	A2TAtAPMx80	B2TAtAPMx20	B2TAtAPMx50	B2TAtAPMx80
A2TAtAPMn20	A2TAtAPMn50	A2TAtAPMn80	B2TAtAPMn20	B2TAtAPMn50	B2TAtAPMn80
A2TAtAPA20	A2TAtAPA50	A2TAtAPA80	B2TAtAPA20	B2TAtAPA50	B2TAtAPA80

The averaged observed runoff for the Nuranang watershed for the simulation years 2004, 2005, 2008, and 2009 were considered as the baseline flow. Taking the same simulation period (17^{th}April-21^{st} August), daily average runoff for the years 2004, 2005, 2008, and 2009, and for each of the 27×6 combinations were determined and percentage change in runoff with respect to the present runoff or baseline flow were estimated.

Performance Indicators

To evaluate the performance of SDSRM, predicted discharges were compared with the observed ones. The performance can be visually interpreted by plotting the simulated and observed data simultaneously on a single plot.

Two dimensionless statistical performance criteria, viz., modelling efficiency (ME) and coefficient of residual mass (CRM) were used as:

$$ME = \frac{\left[\sum_{i=1}^{n_d}(O_{v,i}-\bar{O}_v)^2-\sum_{i=1}^{n_d}(P_{v,i}-O_{v,i})^2\right]}{\sum_{i=1}^{n_d}(O_{v,i}-\bar{O}_v)^2} \quad (1)$$

$$CRM = \frac{\left[\sum_{i=1}^{n_d} O_{v,i}-\sum_{i=1}^{n_d} P_{v,i}\right]}{\sum_{i=1}^{n_d} O_{v,i}} \quad (2)$$

where, $P_{v,i}$ is the predicted or simulated value; $O_{v,i}$ is the observed value; $\bar{O}_v$ is the average observed value and n_d is the number of data used for evaluation.

For a perfect model, the value of ME is 1.0, i.e., when the simulated values match perfectly with the observed ones. A lower value (close to zero) of ME indicates poor performance of the model and a negative value indicates that the model-simulated values are worse than simply using observed mean. CRM indicates the overall under- or over-estimation of the observed value. For a perfect model, the value of CRM is zero. A positive value of CRM indicates the tendency of the model to under-estimate, whereas a negative value indicates a tendency to over-estimate the observed data.

To evaluate the performance of SDSM, coefficient of determination (R^2) and standard error of estimate (SEE) were used. The coefficient of determination (R^2) is calculated as below:

$$R^2 = \left[\frac{\sum_{i=1}^{n_d}(O_{v,i}-\bar{O}_v)\times(P_{v,i}-\bar{P}_v)}{\sqrt{\left\{\sum_{i=1}^{n_d}(O_{v,i}-\bar{O}_v)^2\times(P_{v,i}-\bar{P}_v)^2\right\}}}\right]^2 \quad (3)$$

The range of values for R^2 is 1.0 (best) to 0.0 (worst). The standard error of estimate (SEE) is calculated as below:

$$SEE = \sqrt{\frac{\sum_{i=1}^{n_d}(O_{v,i}-P_{v,i})^2}{n_d-1}} \quad (4)$$

where, $\bar{P}_v$ is the average simulated value.

3. Results and Discussions

Calibration and validation of SDSRM

Runoff generation of the Nuranang watershed was carried out using the SDSRM. The model was calibrated for the depletion period of 2004 (13th April–21st August) and 2005 (17th April–4th September). Critical temperature and runoff coefficient for snowmelt and rain were calibrated to determine the best possible combination of optimal values using the observed runoff data for comparing with simulated runoff. The best possible value of T_{CRIT} were obtained as 5.0 °C for both the years 2004 and 2005. Better matches were obtained for c_R) as 0.4 and 0.5, and c_S as 0.5 and 0.5 for the years 2004 and 2005, respectively. Then, the model was simulated using the respective best possible set of calibration parameters for each calibration year. Validation of SDSRM was performed for the years 2008 (17th April – 20th September) and 2009 (13th April – 23rd September). Using the average values of calibration

parameters, the model was validated. Table 3 shows that the modelling efficiency (ME) and coefficient of residual mass (CRM) values for the calibration and validation years. As in both the calibration and validation years, ME value is more than 0.6 and CRM is less than 0.2, it shows a satisfactory match between observed and predicted runoff. Fig. 2 shows the time series plots of observed and predicted runoff for the calibration and validation years.

Table 3: Best parameter sets and performance assessment of SDSRM during calibration and validation

Parameter	Calibration Years		Validation Years	
	2004	2005	2008	2009
T_{CRIT}, °C	5.00	5.00	5.00	5.00
c_R	0.40	0.50	0.45	0.45
c_S	0.50	0.50	0.50	0.50
ME	0.619	0.736	0.617	0.640
CRM	0.175	0.074	0.183	0.196

Statistical downscaling of temperature and precipitation

Initial Screening of Predictor Variables from NCEP

The predictor 500 hpa geopotential height is found to have maximum correlation in all the three predictant viz. maximum temperature, minimum temperature and precipitation.

Calibration and Validation of SDSM

The data for 1979–1995 were used for calibration and the data for 1996–2001 were used for validation. In this study, seasons of a year were divided as Summer (June – August), Autumn (September – November), Winter (December – February) and Spring (March – May). The performance evaluation of the calibrated model was done using performance indicators ME, CRM, R^2, and SEE. Table 4 shows the performance of SDSM for the calibration and validation period for T_{max}, T_{min} and precipitation for monthly and seasonal data. For all the predictand, T_{max}, T_{min} and precipitation, monthly data gave better results than the seasonal data in both calibration and validation period.

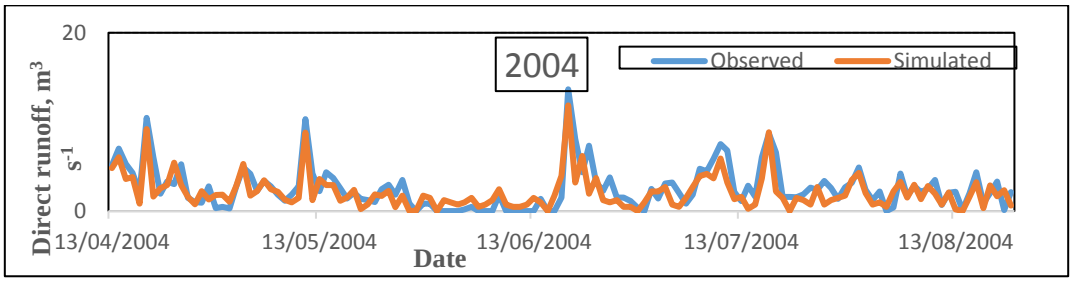

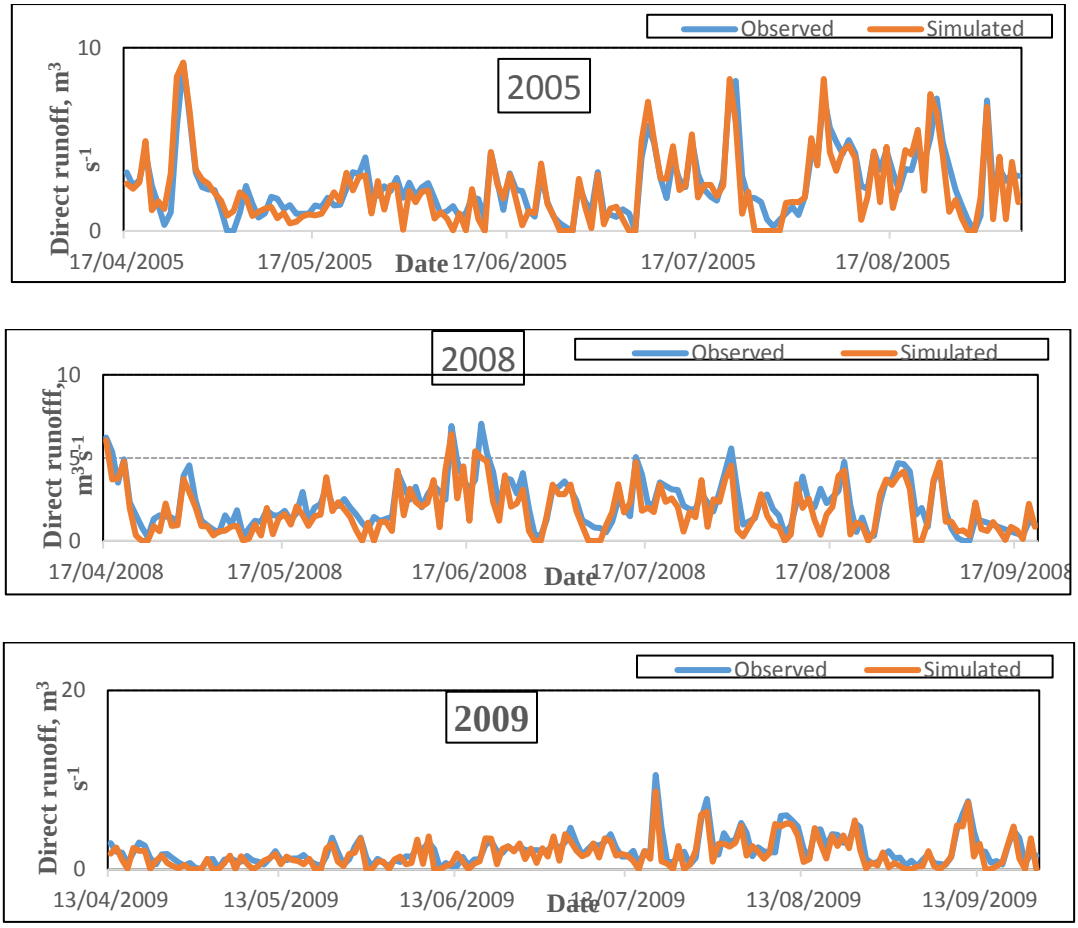

Fig. 2: Time series plots for the calibration and validation years.

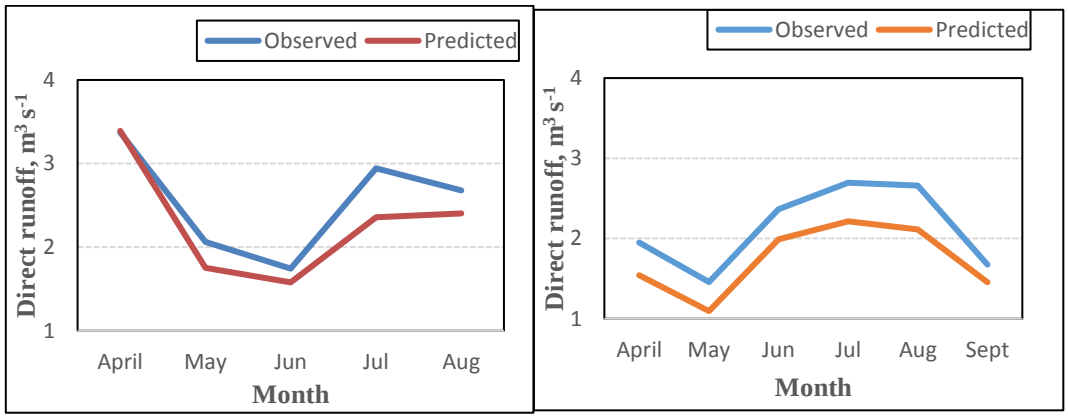

(a) Calibration years (b) Validation years

Fig. 3: Time series plots of monthly average runoff for the calibration (a) and validation (b) years.

Table 4: Performance of SDSM for the calibration and validation period for Tmax, Tmin and precipitation for monthly and seasonal data

Performance criteria	Calibration (1979–1995)			Validation (1996–2001)		
	T_{max}	T_{min}	Precipitation	T_{max}	T_{min}	Precipitation
Monthly						
ME	1.0000	1.0000	0.9999	0.9997	0.9993	0.8555
CRM	0.0000	0.0000	-0.0107	0.0024	0.0054	0.2186
SEE	0.0508	0.0481	0.2400	1.3015	2.0307	3.1575
R^2	1.0000	1.0000	0.9992	0.9998	0.9997	0.9327
Seasonal						
ME	1.0000	1.0000	0.9995	0.9999	0.9998	0.8795
CRM	0.0000	0.0000	-0.0108	0.0024	0.0053	0.2194
SEE	0.0241	0.0212	0.1493	1.0512	1.7708	2.5699
R^2	1.0000	1.0000	0.9999	1.0000	0.9999	0.9910

Assessment of impacts of climate change using the hydrological model

From the 20 generated ensembles of daily temperature (maximum and minimum) from SDSM, monthly average values of maximum temperature (T_{max}), minimum temperature (T_{min}) and precipitation (P) for the time periods 2020s, 2050s and 2080s under both A2 and B2 emission scenarios were determined. Also, the change in T_{max} (°C), T_{min} (°C), and P (%)for each month for each future time periods corresponding to the baseline period were determined. Then, the projected annually averaged change values of the 20 ensembles of of T_{max} (°C), T_{min} (°C), and P (%) with its maximum (*Max*), minimum (*Min*) and average (*Average*) value for the time periods 2020s, 2050s and 2080s under A2 and B2 scenarios respectively were computed. Table 5 shows the maximum, minimum, and average of the projected yearly average change values of T_{max}, T_{min}, and P for the future time periods 2020s, 2050s, and 2080s under A2 and B2 scenarios. From this table, it can be observed that both TA and tA are found to be increasing with the future time period under A2 and B2 scenarios. The TA and tA were found to be maximum in the time period 2080s under A2 scenario with 3.44 and 3.97 °C increase, respectively; while the minimum TA and tA were found in the time period 2020s under B2 scenario with 0.92 and 1.11 °C increase, respectively. Under both the scenarios A2 and B2, the PA were found to be decreasing in the time period 2050s compared to 2020s, then from 2050s, it increased in the time period 2080s. The maximum PA was observed in the time period 2080s under A2 scenario with 12.49% and the minimum PA was observed in the time period 2050s under A2 scenario with -4.63%. The average increase in precipitation under A2 scenario was projected to vary from -0.82 to 12.49% and under B2 scenario from 1.18 to 10.64% considering all the future time periods.

Altogether 27 different combinations of TMx, TMn, TA, tMx, tMn, tA, PMx, PMn, and PA were established for the future periods 2020s, 2050s, and 2080s under A2 and B2 scenarios (Table.2). The values of the nine variables TMx, TMn, TA, tMx, tMn, tA, PMx, PMn, and PA were applied to the daily average observed T_{max}, T_{min}, and P values for simulation years

2004, 2005, 2008, and 2009. Considering these changed values, runoff from the Nuranang watershed was simulated using SDSRM for the 27 combinations for future periods 2020s,

Table 5: Maximum, minimum, and average values of T_{max}, T_{min}, and P for future periods under A2 and B2 scenarios

		A2			B2		
		2020s	**2050s**	**2080s**	**2020s**	**2050s**	**2080s**
T_{max}	Max (TMx)	1.17	2.14	3.61	1.02	1.81	2.29
(°C)	Min (TMn)	0.88	1.95	3.32	0.79	1.51	2.00
	Average (TA)	1.03	2.05	3.44	0.92	1.69	2.13
T_{min}	Max (tMx)	1.31	2.68	4.09	1.22	1.88	3.04
(°C)	Min (tMn)	1.10	2.42	3.87	1.03	1.61	2.81
	Average (tA)	1.20	2.59	3.97	1.11	1.79	2.92
P	Max (PMx)	5.22	2.79	16.79	8.61	5.78	14.62
(%)	Min (PMn)	-10.9	-13.44	6.56	-5.94	-12.12	7.01
	Average (PA)	-0.82	-4.63	12.49	1.18	-2.59	10.64

2050s, and 2080s under A2 and B2 scenarios. For the same simulation period (17th April – 21st August), daily average runoff for years 2004, 2005, 2008, and 2009 were simulated using SDSRM and considered as the present runoff for the baseline period.

For each of the 27 combinations under A2 and B2 scenarios for the future periods 2020s, 2050s, and 2080s, total runoff simulated from the watershed using SDSRM were compared with the present total runoff. Maximum, minimum, and mean runoff volumes were calculated from the 27 combinations of total runoff at the watershed outlet. The change in total runoff (%) were calculated for each of the 27 combinations for future periods of 2020s, 2050s, and 2080s under A2 and B2 scenarios, with respect to the baseline values of total runoff. Tables 6 shows the percent change in total runoff for the 27 combinations for future periods 2020s, 2050s, and 2080s under A2 and B2 scenarios. From Table 7, it can be observed that in 2020s, the mean changes in total runoff are predicted to be -0.81% and 7.46% under A2 and B2 scenarios, respectively. In 2050s, the predicted mean changes in total runoff were found to be -3.22% and -4.27% under A2 and B2 scenarios, respectively. In 2080s, the mean changes in total runoff were predicted as 21.21% and 15.20% under A2 and B2 scenarios, respectively. Under A2 and B2 scenarios, the changes in total runoff were observed to decrease in the future time period 2050s compared to 2020s, then from 2050s, it increased in the future Table 7 Percentage change in total runoff for the 27 combinations for 2020s, 2050s, and 2080s under A2 and B2 scenarios. This same trend was observed in the findings of Mahmood and Jia (2016) where they projected the total runoff for the future years over the Jhelum river basin of Pakistan and India. The mean values of the predicted total runoff obtained from the 27 combinations were plotted on monthly basis for the baseline and future periods by taking daily averages for A2 and B2 scenarios, as shown in Fig. 4. From this Fig. 4, it can be seen

that under both A2 and B2 scenarios, the mean predicted runoff in all the future periods are highest and lowest in April and May, respectively. Under A2 scenario, the mean predicted runoffs in the future periods 2020s and 2050s were found to be higher than the baseline period in the month of April; while they almost matched with baseline in May before increasing again. The mean predicted runoffs in the future period 2080s were much higher than the baseline and the other future periods. Under B2 scenario, the mean predicted runoffs in all the future periods were higher than the baseline, except for 2050s, when it was seen to be slightly lower in June compared to the baseline period. Mean runoffs were predicted maximum in the future period 2080s, followed by 2020s and 2050s.

Table 6: Percent change in total runoff for future periods under A2 and B2 scenarios.

	A2			**B2**		
Combination	**2020s**	**2050s**	**2080s**	**2020s**	**2050s**	**2080s**
1	8.20	9.48	26.06	10.34	10.47	21.34
2	-6.09	-4.91	17.00	-1.14	-5.39	13.96
3	2.84	2.90	20.95	5.15	3.05	17.18
4	7.90	9.10	25.75	11.41	10.08	21.00
5	-6.39	-5.29	16.68	-1.45	-5.79	13.63
6	-0.43	2.52	21.94	4.84	2.66	16.84
7	8.05	9.35	25.89	11.54	10.34	21.16
8	-6.24	-5.04	16.82	-1.32	-5.52	13.79
9	2.70	2.77	22.08	4.97	2.92	17.00
10	7.77	9.20	25.65	11.35	10.03	20.95
11	-6.51	-5.19	16.58	-1.52	-5.83	17.05
12	2.42	2.62	21.83	4.78	2.61	16.79
13	7.48	7.09	25.45	11.04	9.64	20.67
14	-6.81	-1.85	16.38	-1.83	-6.23	13.29
15	2.13	2.39	21.64	4.47	2.22	10.98
16	7.63	9.07	25.47	11.17	9.90	20.81
17	-6.66	-5.32	16.40	-1.70	-5.96	13.43
18	2.27	2.49	21.66	4.60	2.48	16.65
19	7.91	9.35	25.82	11.56	10.30	21.12
20	-6.38	-5.04	16.75	-1.31	-5.57	13.74
21	2.56	2.77	22.01	4.99	2.88	16.96
22	4.49	8.97	25.50	11.25	9.90	20.83
23	-9.80	-5.42	16.43	-1.61	-5.96	13.45
24	-0.86	2.39	21.69	4.68	2.48	16.67
25	4.54	2.18	25.65	11.38	10.17	13.83
26	-9.75	-5.17	16.58	-1.49	-5.70	13.59
27	-0.82	2.64	21.83	4.81	-2.84	16.81
Max	**8.20**	**20.48**	**26.06**	**23.79**	**15.78**	**39.15**
Min	**-9.82**	**-26.93**	**16.36**	**-8.86**	**-15.79**	**-4.96**
Mean	**-0.81**	**-3.22**	**21.21**	**7.46**	**-4.27**	**15.20**

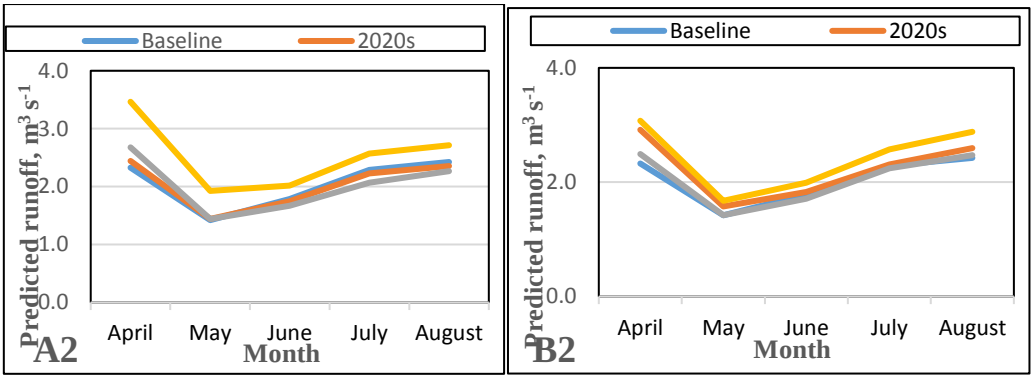

Fig. 4: Monthly plots of mean predicted runoff for baseline and future periods under A2 and B2 scenarios.

Tables 7 show the statistics of present and projected mean discharges, respectively, at the outlet of the watershed under A2 and B2 scenarios. Using this table, box plots were prepared for mean values for baseline and future periods under A2 and B2 scenarios, as shown in Figs. 5. From Fig. 5, it can be seen that under A2 scenario, the predicted mean runoff increased slightly in the future period 2020s as compared to the baseline period, after which it decreased in 2050s and then again increased. Under B2 scenario, the mean predicted runoff decreased in 2020s as compared to baseline period and after that it gradually increased in 2050s and 2080s. The predicted runoff was highest as 6.74 $m^3 s^{-1}$ in the future period 2080s and lowest as 0.42 $m^3 s^{-1}$ in the future period 2050s under A2 scenario.

Table 7: Statistics showing the present and projected mean discharges

Statistics ($m^3 s^{-1}$)	**Baseline**	**2020s**		**2050s**		**2080s**	
		A2	**B2**	**A2**	**B2**	**A2**	**B2**
Mean	1.98	1.97	2.13	1.92	1.98	2.40	2.32
SD	0.87	0.87	0.88	0.75	0.87	1.07	0.98
Minimum	0.45	0.43	0.83	0.42	0.44	0.50	0.76
1st Quartile	1.28	1.28	1.44	1.33	1.26	1.61	1.54
Median	1.87	1.82	1.95	1.78	1.88	2.22	2.24
3rd Quartile	2.53	2.57	2.69	2.37	2.56	3.07	2.87
Maximum	5.60	5.71	4.54	4.27	4.85	6.74	5.39

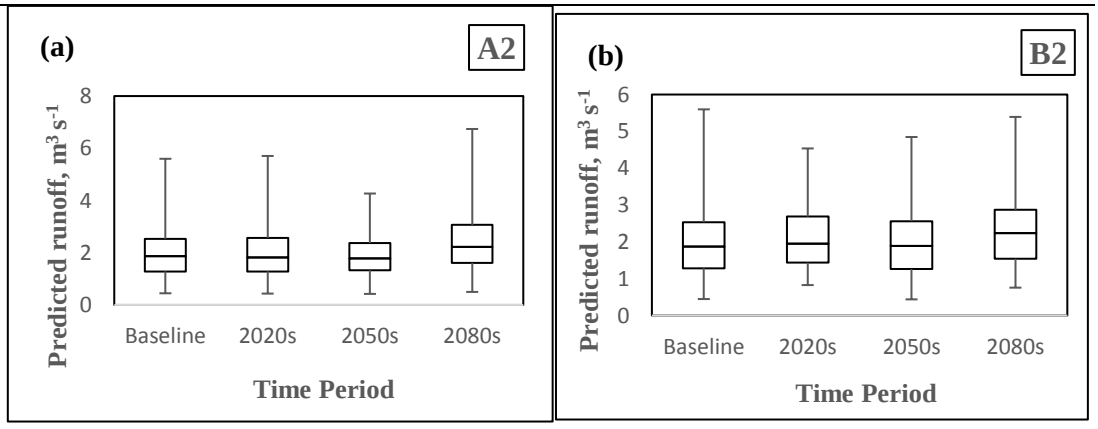

Fig.5 Box plots of mean runoffs for baseline and future periods under (a) A2 and (b) B2 scenarios.

4. Conclusions

The present study was carried out to create a hydrological model of the Nuranang watershed situated in Tawang district of Arunachal Pradesh, India and assess the impact of climate change on the hydrology of the watershed. The hydrology of the watershed was modelled quite well using the SDSRM as it was seen a satisfactory match between observed and predicted runoff with ME value more than 0.6 and CRM less than 0.2, in both the calibration and validation years. Using SDSM, the climate variables obtained as output from a coarser resolution GCM, HadCM3 model was downscaled to obtained finer resolution inputs required by the hydrological model. The initial screening of predictor variable of SDSM resulted the predictor 500 hpa geopotential height to have maximum correlation in all the three predictant viz. maximum temperature, minimum temperature and precipitation. The performance of SDSM for the calibration and validation period for T_{max}, T_{min} and precipitation shows that monthly data gave better results than the seasonal data in both calibration and validation period. The projected change in maximum temperature (T_{max}) showed an increasing trend in the future years. The average increase in T_{max} was projected to vary from 1.03 to 3.44 °C under A2 scenario and from 0.92 to 2.13 °C under B2 scenario in the three future periods. The average increase in minimum temperature (T_{min}) was projected to vary from 1.20 to 3.97 °C under A2 scenario and from 1.11 to 2.92 °C under B2 scenario in all the future periods. The average increase in precipitation was projected to vary from -0.82 to 19.02% under A2 scenario and from 1.18 to 17.05% under B2 scenario in all the future periods. Percent change in total runoff for different future years followed the same trend as change in precipitation from the present climate under both A2 and B2 scenarios. The predicted changes in total runoff were observed as -0.81, -3.22, and 21.21% under A2 scenario for the future years 2020s, 2050s, and 2080s, respectively. Under B2 scenario, the predicted changes in total runoff were observed as 7.46, -4.27, and 15.20% for the future years 2020s, 2050s, and 2080s, respectively. The percentage reduction in total runoff was more in 2050s relative to 2020s, and then it increased again in 2080s.

References

Bandyopadhyay. A., Bhadra, A., Maza, M. and Shelina, R. K. (2014). Monthly variations of air temperature lapse rates in Arunachal Himalaya. *Journal of Indian Water Resources Society*, 34(3), 16–25.

Dibike Y. B. and Coulibaly, P. (2005). Downscaling precipitation and temperature with temporal neural networks. *American Meteorological Society*, 6, 483–496.

Fowler, H. J., Blenkinsop, S. and Tebaldi, C. (2007). Linking climate change modelling to impacts studies: Recent advances in downscaling techniques for hydrological modelling. *International Journal of Climatology*, 27, 1547–1578.

Harpham C. and Wilby R. L. (2005). Multi-site downscaling of heavy daily precipitation occurrence and amounts. *Journal of Hydrology*, 312, 235–255.

IPCC. 2014. Climate Change (2014): Synthesis Report. Contribution of Working Groups I, II and III to the Fifth Assessment Report of the Intergovernmental Panel on Climate Change (IPCC), R.K. Pachauri and L.A. Meyer (Eds.)., Geneva, Switzerland.

Kabiri, R., Bai, V. R. and Chan, A. (2015). Assessment of hydrologic impacts of climate change on the runoff trend in Klang watershed, Malaysia. *Environmental Earth Science*, 73(1), 27–37.

Liu, L., Liu, Z., Ren, X., Fischer, T. and Xu, Y. (2011). Hydrological impacts of climate change in the Yellow river basin for the 21st century using hydrological model and statistical downscaling model. *Quaternary International*, 244(2), 211–220.

Mahmood, R. and Jia, S. (2016). Assessment of impacts of climate change on the water resources of the transboundary Jhelum river basin of Pakistan and India. *Water*, 246(8): 1–18.

Raghunath, H. M. (2006). Hydrology principle, analysis, design. New Age International (P) Ltd., New Delhi, India. 407–412.

Schubert, S. and Sellers, A. H. (1997). A statistical model to downscale local daily temperature extremes from synoptic-scale atmospheric circulation patterns in the Australian region. *Climate Dynamics*, 13, 223–234.

Shrestha, A. B. and Devkota, L. P. (2010). Climate change in the Eastern Himalayas: Observed trends and model projections; Climate change impact and vulnerability in the Eastern Himalayas – Technical Report 1. Kathmandu: ICIMOD.

Wilby R. L, Wigley T. M. L., Conway, D., Jones, P. D., Hewitson, B. C., Main, J., and Wilks, D. S. (1998). Statistical downscaling of general circulation model output: A comparison of methods. *Water Resources Research*, 34(11), 2995–3008.

Wilby, R. L. and Wilks D. S. (1999). The weather generation game: A review of stochastic weather models. *Progress in Physical Geography*, 23, 329–357.

Wilby, R. L., Dawson C. W. and Barrow E. M. (2002). SDSM — a decision support tool for the assessment of regional climate change impacts. *Environmental Modelling and Software*, 17, 147–159.